Pioneer. Adv. Mater. 2026, 1(2): 1-10 *DOI: 10.48308/piadm.2025.241222.1007*

Shahid Beheshti University

Pioneering Advances in Materials

Journal homepage: http://piadm.sbu.ac.ir ISSN: 3115-7114

Research paper

Zinc Oxide Nanoparticles and Tyrosine Hydroxylase: Structural, Functional, and Cytotoxic Interactions with Implications for Parkinson's Disease

Paria Kamali [1], ***Fateme Mirzajani*** [1,2,3,*]

[1] ***Protein Research Center, Shahid Beheshti University, Tehran, Iran***

[2] ***Faculty of Life Sciences and Biotechnology, Shahid Beheshti University, Tehran, Iran***

[3] ***Department of Medical laboratory science, College of Science, Knowledge University, Kirkuk Road, Erbil, Iraq***

[*] *f_mirzajani@sbu.ac.ir*

Article info:

Article history:

Received: 29/08/2025

Accepted: 31/08/2025

Keywords:
Zinc oxide nanoparticles, Tyrosine hydroxylase, Parkinson's disease, Neurotoxicity, Protein corona.

Abstract

Nanoparticles have impact in biomedical science due to their physical, chemical, and biological characteristics. Amongst, Zinc oxide nanoparticles (ZnO NPs), have been extensively studied for their applications in drug delivery, biosensing, and neuroprotection. However, the neurotoxicity and disruption of enzyme-based reactions have been controversial. In the present work, chemically synthesized ZnO NPs were characterized using UV–Vis spectroscopy, X-ray diffraction (XRD), dynamic light scattering (DLS), and scanning electron microscopy (SEM). Bio-interaction of ZnO NPs with tyrosine hydroxylase (TH), a rate-limiting enzyme for dopamine biosynthesis, was estimated by circular dichroism (CD) spectroscopy, ELISA-based activity assays, and SDS-PAGE for protein corona analysis. Cytotoxicity in PC12 neuronal cells was studied using MTT and live/dead staining. Results indicated ZnO NPs altered TH secondary structure (56.4 %), notably inhibited enzyme activity (56.4 %), and induced dose-dependent toxicity (IC_{50} value of 0.312 µg/mL). These findings suggest ZnO NPs have a bivalent role in neurobiology: as potential medications, but uncontrolled exposure will exacerbate neuronal damage and Parkinson's disease progression.

1. Introduction

Nanotechnology, which is the manipulation of material in the 1–100 nm scale, has transformed many fields, specifically biomedicine, electronics, and environmental sciences. Nanoparticles (NPs) have distinctive characteristics that make them useful for drug delivery, bioimaging, biosensors, and neurotherapeutic interventions (1). Some of the characteristics of the nanoparticles are their enhanced surface-to-volume ratio, ability to

change size, and ability to pass through biological barriers. Zinc oxide nanoparticles (ZnO NPs) have attracted much attention among many of the nanoparticles due to their broad antimicrobial activity, photocatalytic activity, chemical stability, and possible biocompatibility (2). Also, ZnO NPs are fairly inexpensive to synthesize, and can be prepared with defined shapes and surface features, making them very useful in biomedical fields.

Though these applications are promising, there is some dispute over the interactions of ZnO NPs with biological systems. ZnO NPs are also shown to produce ROS, and at elevated concentration, they are capable of inducing oxidative stress, inflammation, and DNA damage (3). At controlled concentration, ZnO nanoparticles have also exhibited useful properties like antimicrobial activity and cell signaling modulation. The binarity of ZnO NPs underscores the need for considering their dose-dependent activity on targeted biomolecular entities, particularly in the nervous system (3).

Alzheimer's disease, Huntington's disease, and Parkinson's disease (PD) are all neurodegenerative disorders that are serious health disorders worldwide (4, 5).

PD is the second most prevalent neurodegenerative disease that affects more than 10 million individuals worldwide (5). The illness is marked by progressive degeneration of dopaminergic neurons of substantia nigra pars compacta, leading to lowering of dopamine in the striatum. The clinical manifestations are tremor, bradykinesia, rigidity, and postural instability (6, 7). Current treatment strategies are predominantly centered on dopamine replacement therapy, which also involves the use of L-DOPA; however, these therapies do not halt disease progression and have complications on a long-term basis(8). Tyrosine hydroxylase (TH) is a key enzyme in dopamine biosynthesis. It catalyzes the transformation of L-tyrosine into L-DOPA, the immediate precursor of dopamine (9, 10). Phosphorylation, cofactors like tetrahydrobiopterin, and negative feedback from catecholamine levels all work together to strictly regulate TH activity. Inhibition or dysregulation of TH leads to a deficiency of dopamine and progression of Parkinson's disease directly (11). As such, any factor that can change TH function or structure can very much influence the dopaminergic system.

Recent research indicates that nanoparticles, specifically ZnO NPs, may interact with enzymes by inducing conformation changes, inhibition, or even activation, depending on size, charge, and concentration (12). It previously mentioned that the ZnO NP-induced apoptosis in neuronal cells through oxidative stress.

Also ZnO NPs are prone to protein coronas formation in biological systems, which modifies their bioactivity (13).

These observations pose significant questions regarding the capacity of ZnO NPs to influence enzymes central to neurological function, including TH. Therefore, in the current study, it is desired to reveal systemically the influence of ZnO nanoparticles on the structure, activity, and cell effect of TH (14).

This study is unlike any of the past research since it represents the first systematic investigation of the direct interaction between ZnO nanoparticles and tyrosine hydroxylase (TH), a rate-determining enzyme in dopamine biosynthesis with central implications in Parkinson's disease pathology.

While ZnO NPs have been already studied for their general cytotoxic, antimicrobial, or neuroprotective activities, enzyme-specific structural and functional effects on TH have not been properly investigated. By combining biophysical (CD spectroscopy), biochemical (ELISA activity), and protein adsorption (SDS-PAGE) analyses with neuronal cytotoxicity assays, our investigation provides a unique molecular-to-cellular scale perspective of ZnO–TH interactions. This integrated approach highlights the possibility of ZnO NPs to both disrupt neuronal enzyme activity and induce dose-dependent toxicity, thereby yielding mechanistic insight into the ways nanoparticles may play a role in or exacerbate dopaminergic dysfunction in Parkinson's disease.

In this study ZnO NPs characterize using various physicochemical methods, investigate structural transition in TH by CD spectroscopy, measure enzymatic activity by ELISA assays, analyze protein corona formation by SDS-PAGE, and analyze cytotoxicity on PC12 neuronal cells by MTT and live/dead staining assays.

The study provides novel evidence of bimodal activity of ZnO nanoparticles in neurobiology

and application in Parkinson's disease by integrating molecular, biochemical, and cellular investigations.

2. Materials and Methods

2.1. Reagents and Chemicals

Merck (Germany) supplied zinc acetate dihydrate [$Zn(CH_3COO)_2 \cdot 2H_2O$], sodium hydroxide (NaOH), absolute ethanol, and phosphate-buffered saline (PBS, pH 7.4). Tyrosine hydroxylase (recombinant rat enzyme) and ELISA kit for the activity assay were Sigma-Aldrich (USA) products. Cell culture reagents like Dulbecco's Modified Eagle's Medium (DMEM), fetal bovine serum (FBS), penicillin-streptomycin (100 U/mL), and trypsin-EDTA were supplied by Gibco (USA). PC12 neuronal cells were donated by the Pasteur Institute of Iran, gratefully. Chemicals were of analytical grade and used without purification.

2.2. Preparation of ZnO Nanoparticles

ZnO nanoparticles were prepared by chemical precipitation. Typically, 0.1 M zinc acetate dihydrate was dissolved in 100 mL of absolute ethanol at room temperature (25 °C) under stirring. A 0.2 M solution of NaOH in ethanol was prepared and was added slowly (1 mL/min) to the zinc acetate solution in a well-stirred state at 800 rpm. The reaction mixture was stirred at 60 °C for 2 h until it became white precipitated. The precipitate was centrifuged at 10,000 rpm for 15 minutes, washed three times with ethanol and deionized water to remove the impurities from the sample and dry over the course of one night at 80 °C in a hot-air oven. The ZnO nanopowder thus obtained was calcined at 400 °C for 2 h in a muffle furnace for improving crystallinity. The powder was kept in airtight vials and stored for future use. The ZnO nanopowder obtained was calcined at 400 °C for 2 h in a muffle furnace to improve crystallinity. The powder was kept in airtight vials for further use.

2.3. Statistical Analysis

Design Expert software (version 7.0.0, Minneapolis, USA) was utilized to design experiments and analyze data. This software is specifically used to optimize experimental parameters and investigate the interaction effects of more than one factor.

Table 1: Quantitative and designed factors of each of them, α was ±1.5406.

Quantitative Factors	Unit	+α	1	0	-1	-α
Time	min	220	180	120	60	20
Nanoparticle/Enzyme Conc.	µg/mL	30	25	16.5	7.5	1.5
Enzyme Concentration	%	370	300	200	100	32

In designing experiments, the central composite design (CCD) method has been used because its orthogonal and rotational nature facilitates accurate analysis. This technique enables the observation of interaction effects of factors with a small number of repeated experiments and facilitates the plotting of the results as two-dimensional and three-dimensional graphs. In this case, three quantitative factors were considered, e.g., nanoparticles to enzyme ratio (based on 1 mg of enzyme per ml), time of treatment, and enzyme concentration. One quality factor, the type of nanoparticle (zinc oxide nanoparticles), was also incorporated in the design. The value of α was 1.5406 and the experiments were at five levels for each factor with 20 different treatments suggested by the software (Tables 1 and 2).

Table 2: Experiments designed based on factors and enzyme response.

No.	Time (min)	Nanoparticle Ratio (%)	Enzyme Concentration (ng)	Enzyme Activity
1	120	16.5	32	7.5922
2	60	25	300	7.4579
3	60	7.5	300	7.3958
4	180	25	370	7.3661
5	120	16.5	200	7.0643
6	120	16.5	200	7.4885
7	120	1.5	200	7.7024
8	120	30	200	7.5302
9	120	16.5	200	7.6563
10	180	25	100	7.0495
11	60	7.5	100	7.5159
12	180	7.5	300	7.4256
13	20	16.5	200	7.4021
14	180	7.5	100	7.3941
15	120	16.5	200	7.0485
16	60	25	100	7.6457
17	120	16.5	200	7.0492
18	120	16.5	200	7.3895
19	220	16.5	200	7.4945
20	120	16.5	200	7.5509

All the experiments were performed in triplicate (n = 3). The data are presented as mean ± SD. One-way ANOVA with statistical test was applied to compare the treatment groups, and regression analysis was applied to dose–response modeling of enzyme inhibition and cytotoxicity. IC_{50} values with 95% confidence intervals were determined using nonlinear regression (four-parameter logistic model). Statistical significance was accepted to be at $p < 0.05$.

2.4. ZnO Nanoparticle Characterization

UV–Vis Spectroscopy: Optical properties of ZnO NPs were examined by a UV–Vis spectrophotometer (Shimadzu UV-2600). ZnO NPs dispersions in ethanol (0.1 mg/mL) were scanned from 200 to 800 nm with a resolution of 1 nm. For the X-ray Diffraction (XRD), crystal structure was determined with an X-ray diffractometer (Bruker D8 Advance, Cu-Kα radiation, λ = 1.5406 Å). Data were recorded between 20°–80° (2θ) with a step size of 0.02°. Crystallite size was determined using the Scherrer equation. The zeta Potential and Dynamic Light Scattering (DLS) results showed the hydrodynamic size distribution and the surface charge were characterized by Malvern Zetasizer Nano ZS90. The samples were dissolved in deionized water at the concentration of 0.5 mg/mL. Finally, the scanning Electron Microscopy (SEM): Morphology was characterized by SEM (Hitachi S-4700). Samples were coated with a thin layer of gold prior to imaging.

2.5. Characterization of Tyrosine Hydroxylase

• *Tyrosine Hydroxylase @ ZnO NPs Treatment:* Tyrosine hydroxylase was dispersed in PBS (pH 7.4) at 0.5 mg/mL. ZnO NPs were sonicated (15 min, 40 kHz, 100 W) for dispersal in PBS at different concentrations (0, 10, 25, 50, 100 μg/mL) to avoid agglomeration. Protein solution and suspensions of ZnO NP of the same volume were incubated at 37 °C for 1 h by slow shaking. Functional and structural studies were performed with treated samples.

• *Circular Dichroism (CD) Spectroscopy:* TH secondary structure changes were probed in a Jasco J-810 spectropolarimeter. Protein-NP complexes were formed in 0.2 mg/mL protein concentration. Far-UV CD spectra were recorded in the range 190–260 nm at 25 °C in a 0.1 cm path length quartz cuvette. The mean of three scans was buffer baseline-corrected spectrum. Data were expressed as mean residue ellipticity (MRE) and evaluated for α-helix, β-sheet, and random coil composition prediction with the CDPro software package.

• *Activity Assay:* The catalytic activity of TH with and without ZnO NPs was measured quantitatively using an ELISA-based kit (Sigma, USA).

• *Activity Assay:* Quantitatively, the catalytic activity of TH with and without ZnO NPs was determined by ELISA-based kit (Sigma, USA). The enzyme solution (50 μL) was mixed with variable concentrations of ZnO NPs (0-100 μg/mL) for 1 h at 37 °C. Catalytic activity was triggered after adding substrate L-tyrosine and cofactor tetrahydrobiopterin. At 30 min, reaction mixture was prepared following kit procedure and read at 450 nm in microplate reader (BioTek Synergy HT). Enzyme activity was expressed relative to untreated control (100%).

• *SDS-PAGE analysis of the protein corona:* Adsorption and potential protein corona formation on ZnO NPs was determined by SDS-PAGE. The same samples were centrifuged at 15,000 rpm for 20 min following 1 h incubation of TH with ZnO NPs (50 μg/mL) at 37 °C. The pellet (protein-NP complex) was washed with PBS and dissolved in Laemmli buffer. Supernatant and pellet were both boiled in 95 °C water for 5 min and resolved on 12% polyacrylamide gel electrophoresis. Gels were stained with Coomassie Brilliant Blue and recorded in a gel recording system.

• *MTT Assay and Cell Culture and Cytotoxicity Assays***:** PC12 neuronal cells were cultured in DMEM medium that contained 10% FBS, 1% penicillin-streptomycin, and 1% L-glutamine. Incubation at 37 °C was performed in a 5% CO_2 humidified environment. Subculturing was performed every two weeks. Cell viability was measured by the MTT assay. Short-term, 1×10^4 cells/well were seeded onto 96-well plates and allowed to incubate overnight. ZnO NPs were exposed to 0, 1, 5, 10, 25, 50, and 100 μg/mL for 24 h. After exposure, 20 μL of MTT solution (5

mg/mL PBS) was added to every well and incubated for 4 h. 150 µL DMSO was used for the solubilization of formazan crystals and read at 570 nm using a microplate reader. Cell viability was presented as percentage control no treatment. IC_{50} values were determined by nonlinear regression analysis(15).

• *Live/Dead Cell Staining:* Viability was verified by Calcein-AM (green, live) and propidium iodide (PI, red, dead). PC12 cells were seeded onto coverslips in 24-well plates and treated with ZnO NPs (0, 10, 25, 50 µg/mL) for 24 h. The cells were stained with 2 µM Calcein-AM and 4 µM PI at 20°C in the dark for 20 min and washed with PBS. Fluorescence images were captured by an Olympus IX71 inverted fluorescence microscope (16).

3. Results

This research was aimed at exploring the physicochemical characteristics and biological activities of ZnO NPs synthesized via a sequence of spectroscopic, microscopic, and biochemical processes.

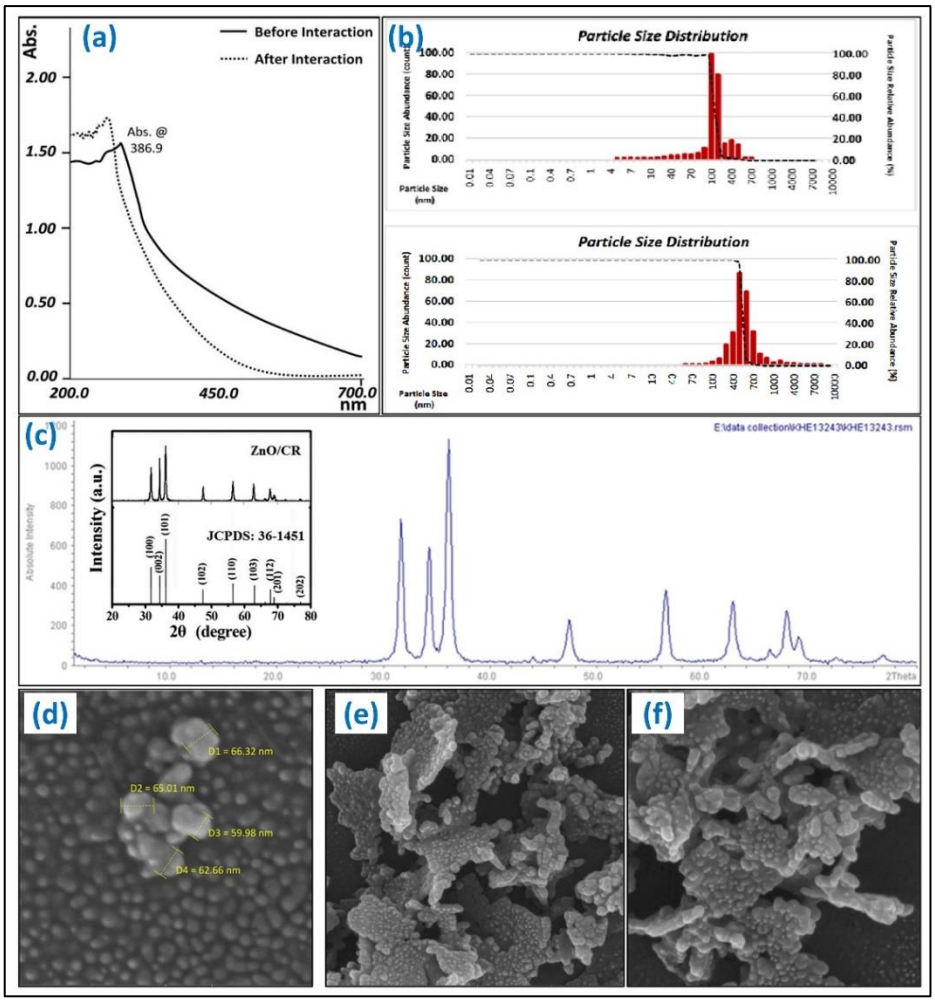

Figure 1: Characterization of ZnO Nanoparticles based on physical and chemical properties: Absorption of zinc oxide nanoparticles at a wavelength of 200 to 700 nm before and after interaction with the enzyme (a), size distribution of zinc oxide nanoparticles before and after interaction with the enzyme (b), investigation of the crystalline structure of zinc oxide nanoparticles at different angles using XRD (c), image of zinc oxide nanoparticles using an electron microscope before interaction with the enzyme (d) and after interaction with the enzyme (e and f).

We first ZnO structural and morphological analyses. Then, their interaction with tyrosine hydroxylase was investigated at both structural and functional levels. Second, the process of protein corona formation was taken into account. Finally, cytotoxicity of ZnO NPs against neuronal PC12 cells was studied to determine their biological relevance.

3.1. Characterization of ZnO Nanoparticles Based on Physical and Chemical Properties

ZnO NPs UV–Vis Spectroscopy (Figure 1a), showed a sharp absorption peak at around 365 nm, characteristic of the intrinsic band-gap absorption of ZnO since electrons from the valence band are being excited to the conduction band. The sharpness of the peak confirmed the crystalline nature of the nanoparticles and that aggregation was minimal. Synthesis of ZnO NPs with specified optical properties was demonstrated. The XRD pattern of ZnO NPs (Figure 1c) showed sharp diffraction peaks at 2θ = 31.7°, 34.4°, 36.2°, 47.5°, 56.6°, and 62.8°. These correspond to the (100), (002), (101), (102), (110), and (103) planes of hexagonal wurtzite ZnO (JCPDS card no. 361451). No secondary peaks of impurities were observed, which confirms that the sample is highly pure. Upon applying Scherrer's formula, we estimated that the size of crystallites was around 25 nm. SEM micrographs indicated ZnO NPs (Figure d, e and f) to be largely spherical in shape and somewhat agglomerated. This is characteristic of metal oxide nanocrystals because they have a large amount of surface energy. The particle size from SEM images averaged between 20 and 30 nm, which is in agreement with what was obtained by XRD. DLS and Average hydrodynamic diameter by (Figure 1b) DLS Zeta Potential was 55 ± 10 nm, a bit larger than that as seen by SEM. This is attributed to solvation layers and small degrees of aggregation in water. The zeta potential was -23 mV, i.e., biological buffer dispersions are quite stable.

3.2. ZnO NPs influences on the conformation of Tyrosine Hydroxylase

The far-UV CD spectra of TH (Figure 2f) showed two negative minima at 208 and 222 nm, typical of α-helical proteins. On increasing the concentration of ZnO NPs (10–100 μg/mL), ellipticity decreased gradually, especially at 222 nm. Quantitative second structure analysis indicated a reduction in the α-helices content (from 42% to 28%) and an increase in the random coils content simultaneously, thus confirming the partial denaturation of the enzyme. These data proved that ZnO NPs altered the TH conformation depending on the concentration. Regression analysis confirmed the strong dose dependent relationship of ZnO nanoparticle concentration and loss of α-helix, confirming concentration dependent destabilization of TH structure. These are R^2 = 0.92 over $p < 0.001$.

3.3. How ZnO NPs modulate the activity of Tyrosine Hydroxylase

Enzymatic activity ELISA-based assay indicated that ZnO NP treatment (Table 3 and Figure 2a), significantly inhibited TH activity. For 10 μg/mL, activity was approximately 85% of control and at 100 μg/mL merely 40% residual activity. Statistical comparison also confirmed dose-dependent inhibition ($p < 0.01$). This indicated that ZnO nanoparticles not only disrupted the structure of TH but also affected the catalytic activity, which could be able to suppress dopamine biosynthesis in neuronal systems. ANOVA revealed that TH activity was significantly affected by ZnO NP concentration ($F = 2.84$, $P=0.003$, $p < 0.01$), and statistical test confirmed that inhibition at 50 and 100 μg/mL was significantly greater than at 10 μg/mL ($p < 0.05$).

Table 3: Results obtained from analysis of variance to evaluate the effect of various factors on the activity of tyrosine hydroxylase enzyme.

Source	Sum of Squares	df	Mean Square	F-Value	p-Value (Prob>F)
Model	9.16	17	0.54	2.84	0.003*
A-Time	1.32	1	1.32	6.94	0.0117
B-NP ratio	0.57	1	0.57	3.01	0.09
C-Conc.	0.66	1	0.66	3.48	0.0692
AB	0.13	1	0.13	0.7	0.5696
AC	1.25	1	1.25	6.57	0.4778
BC	0.022	1	0.022	0.11	0.0823
Residual	7.97	42	0.19		
Lack of Fit	5.2	27	1.47E-08	1.04	0.482**
R-Squared	0.5346		Adj R-Squared	0.4663	
* Significant	** Not significant				

3.4. Protein Corona Formation

SDS-PAGE Analysis (Figure 2b and 2c): Upon mixing TH with ZnO NPs, the SDS-PAGE patterns confirmed that band intensity in the supernatant fraction was reduced and there was

a clear-cut band for TH in the nanoparticle-bound pellet. This confirmed that TH molecules bound to ZnO NP surfaces, creating a protein corona.

Densitometry scan revealed a significant reduction in free TH bands in the supernatant upon increasing ZnO NP concentration ($p < 0.05$), as would be predicted for dose-dependent protein adsorption. The formation of such a corona may have caused the enzyme to change shape and lose part of its function.

3.5. Toxicity to PC12 Cells

The MTT Assay (Figure 2d and 2e) indicated that ZnO NPs were cytotoxic to PC12 cells in a concentration-dependent manner.

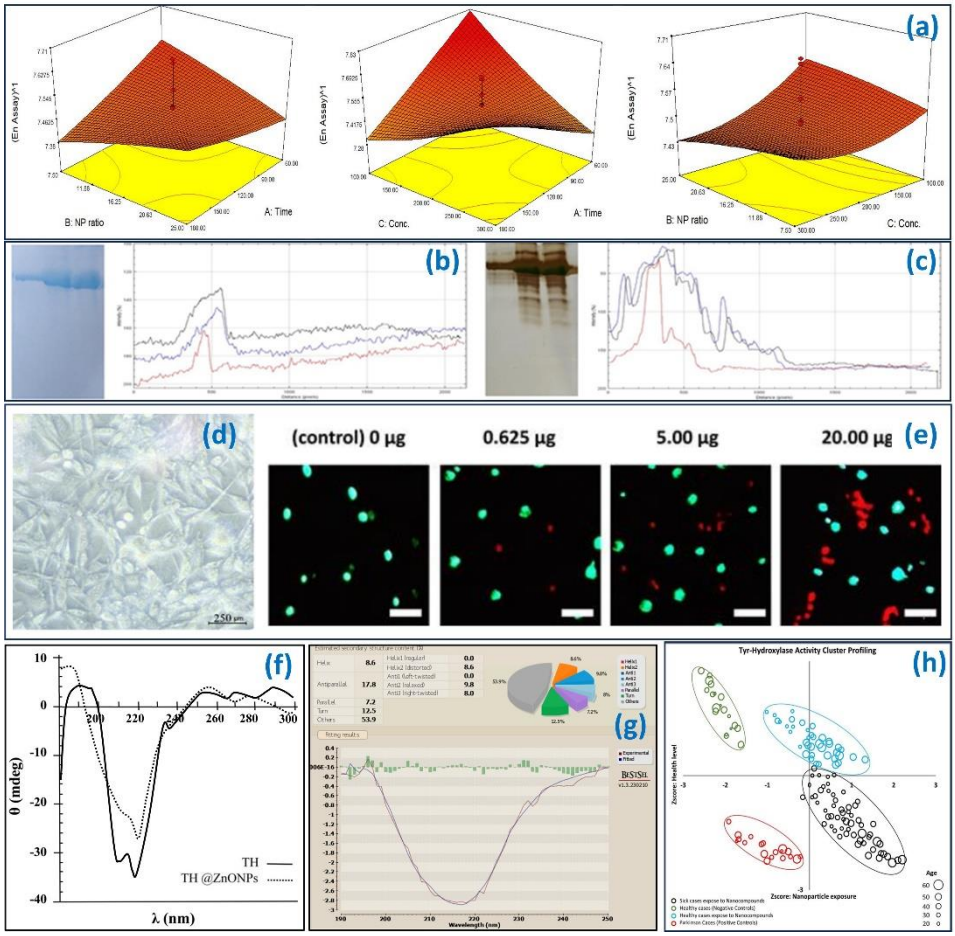

Figure 2: Response surface results of the effect of zinc oxide nanoparticles on the activity of tyrosine hydroxylase enzyme based on binary factors (a), investigation of protein crowns on the surface of zinc oxide nanoparticles by gel electrophoresis with Coomassie brilliant blue staining (b) and with silver nitrate staining (c), phase contrast image of PC12 cells after 24 exposures to zinc oxide nanoparticles (d), images obtained from staining of zinc oxide nanorods at different concentrations (e), CD spectrum of tyrosine hydroxylase enzyme (f), after interaction with zinc oxide nanoparticles and percentage of changes in the secondary structure of this enzyme (g), and investigation of the effect of zinc oxide nanoparticles on the selected group of individuals (h).

The viability of cells was still more than 85% even when the concentration reached 5 µg/mL. The viability reduced to 65% at 25 µg/mL and reached only 28% of cells alive at 100 µg/mL. Nonlinear regression analysis yielded an IC_{50} of 0.312 µg/mL (95% CI: 0.27–0.36 µg/mL; R^2 =

0.95), and ANOVA confirmed a concentration-dependent reduction in viability statistically ($p < 0.001$). Live/dead cell ratios were similarly significantly different between 10 and 50 μg/mL groups (Chi-square test, $p < 0.01$). The IC_{50} value was found to be 0.312 μg/mL, which means that neuronal cells are highly sensitive to ZnO NPs. Live/Dead Cell Staining (Figure 2e): Fluorescence microscopy supported the MTT result. The control cells without treatment contained intensive green fluorescence (Calcein-AM), indicating healthy and living cells. In contrast, groups that were treated with ZnO NP contained more red fluorescence (PI) at increased concentrations, indicating membranes were ruptured and the cells died. At 50 μg/mL treatment, cells shrunk and disintegrated, which were shape changes.

4. Discussion

his study thoroughly assessed the interaction of ZnO nanoparticles and tyrosine hydroxylase (TH) and offered data concerning structural, functional, and cellular consequences. According to our findings, ZnO NPs, which were crystalline in nature and stable, changed the conformation of TH, blocked its activity as an enzyme, and caused apoptosis of neuronal PC12 cells. Physicochemical measurements affirmed the successful preparation of ZnO NPs with spherical shape and nanoscale dimensions. It has been determined that the above features make surfaces more reactive, and that is the reason why they react so vigorously with proteins. It have reported similar findings, whereby ZnO nanoparticles exhibit facile adsorption of plasma proteins to form stable coronas (14, 17). Through our work, SDS-PAGE proved that TH exerts very high binding affinity for ZnO NPs in support of the hypothesis that enzyme adsorption on the surface of nanoparticles has the potential to induce conformational changes and functional damage. The CD spectroscopy readings determined that the concentration of α-helix diminished considerably and that random coil structure concentration was on increase, showing protein unfolding. Similar structural destabilization has been demonstrated in previous work on ZnO NP-protein interactions, e.g., with bovine serum albumin (18). TH is a stringently regulated enzyme where structure is extremely critical in forming dopamine. So, even a little bit of unfolding can cause a loss of activity, which is in line with our ELISA-based results that show dose-dependent inhibition. These effects not only quantitatively reported but also statistically established, with regression and ANOVA ascertaining that ZnO NP concentration was a significant predictor of TH inhibition and neuronal cytotoxicity ($p < 0.01$). From a pathophysiologic viewpoint, the inhibition of TH activity noted here has significant bearing on Parkinson's disease. Dopamine deficiency in Parkinson's disease results from degeneration of dopaminergic neurons, and any external factor further impairing tyrosine hydroxylase (TH) activity might have a chance of advancing disease onset. This concept is reinforced by the findings of our current study where robust inhibition of catalytic TH activity in vitro by ZnO nanoparticles was demonstrated. Cytotoxicity values also determined the sensitivity of the neuronal cell to ZnO nanoparticles. The IC_{50} of 0.312 μg/mL in PC12 cells was significantly lower than that reported in non-neuronal cells like fibroblasts or epithelial lines (19).

which reflects increased sensitivity in neurons. This activity results from oxidative stress, mitochondrion dysfunction, and membrane disruption by ZnO NPs, as previously determined in other research work.The live/dead assay also supported the same observations with a higher percentage of cell death with rising concentration of ZnO NPs.

It is interesting to notice that high concentrations of ZnO NPs were toxic but did not produce significant effects on cell viability and enzyme activity at doses (<5 μg/mL). A bimodal behavior as such hints that ZnO NPs may be designed for useful applications, for example, targeted drug delivery or biosensing, provided their interactions with neuron enzymes are carefully controlled. Surface modifications, e.g., PEGylation or coating with biocompatible polymers, may suppress deleterious protein binding and toxicity (20).

Our findings demonstrate a bimodal function of ZnO NPs: great biomedical potential, yet the uncontrolled nature of the NPs can potentiate neurodegeneration via direct inhibition of TH and disruption of neuronal integrity. This points toward optimization of doses, surface modification, and stringent safety assessment prior to clinical application.

5. Conclusion

In this study, ZnO nanoparticle cytotoxicity and tyrosine hydroxylase and their biological activities toward the neuronal PC12 cells were examined in a systematic manner. Spherical, crystalline, and stable ZnO nanoparticles with the average particle diameter of 20–30 nm were synthesized. Spectroscopic studies revealed that the nanoparticles caused abrupt conformational changes in tyrosine hydroxylase, which were reflected as loss of α-helix content and increase in random coils. This change in conformation led to a dose-dependent enzymatic inactivation, with increasing concentrations leading to a significant loss of catalytic function. The SDS-PAGE analysis also illustrated the formation of a protein corona by tyrosine hydroxylase adsorption onto the nanoparticle surface, which would have resulted in conformational as well as functional modification.

Aside from having direct effects on the enzyme, ZnO NPs were also highly toxic against PC12 neuronal cells with an IC_{50} of 0.312 μg/mL and an impressive decrease in cell viability at higher concentrations. These findings collectively bring to the forefront the two faces of ZnO nanoparticles in neurobiology: their physicochemical properties can hold potential for drug delivery and biosensing applications, but their high affinity for proteins and their acute cytotoxicity express potential hazards to neuronal systems. Future efforts must be aimed at surface modification techniques to reduce protein adsorption, in vivo testing in models of Parkinson's disease, and long-term toxicity studies to determine safe therapeutic windows. In total, this research instructs us on how nanoparticles and enzymes interact and opens the door to the intelligent design of safer nanomedicine strategies to neurodegenerative

6. Declaration of Competing Interest

The authors declare that there is no conflict of interest.

7. Data availability

The processed data used and analyzed during the current study are available from the corresponding author upon reasonable request.

8. Financial support

No grant or financial support was used to conduct this research.

9. Conflict of interest

Authors have no conflict of interest to declare.

References

1. *Gupta RK, Gawad FA El, Ali EAE, Karunanithi S, Yugiani P, and Srivastav PP. Nanotechnology: Current applications and future scope in food packaging systems. Measurement: Food (2024) 13: 100131.*
2. *Naknaen P. Utilization possibilities of antimicrobial biodegradable packaging produced by poly(butylene succinate) modified with zinc oxide nanoparticles in fresh-cut apple slices. Int Food Res J (2014) 21: 2413–2420.*
3. *Shrivastava R, Raza S, Yadav A, Kushwaha P, and Flora SJS. Effects of sub-acute exposure to TiO2, ZnO and Al2O3 nanoparticles on oxidative stress and histological changes in mouse liver and brain. Drug Chem Toxicol [serial online] 2014 [cited 2023 Dec 29], 37: 336–347. Available from: URL: https://pubmed.ncbi.nlm.nih.gov/24344737/*
4. *Chen T-H, Chou M-C, Lai C-L, Wu S-J, Hsu C-L, and Yang Y-H. Factors affecting therapeutic response to Rivastigmine in Alzheimer's disease patients in Taiwan. Kaohsiung J Med Sci (2017) 33: 277–283.*
5. *Lee TK and Yankee EL. A review on Parkinson's disease treatment. Neuroimmunol Neuroinflamm (2022) 8: 222.*
6. *McRae-McKee K, Udeh-Momoh CT, Price G, Bajaj S, de Jager CA, Scott D, et al. Perspective: Clinical relevance of the dichotomous classification of Alzheimer's disease biomarkers: Should there be a "gray zone"? Alzheimer's & Dementia (2019) 15: 1348–1356.*
7. *Finseth TA, Hedeman JL, Brown RP, Johnson KI, Binder MS, and Kluger BM. Self-reported efficacy of cannabis and other complementary medicine modalities by Parkinson's disease patients in Colorado. Evidence-based Complementary and Alternative Medicine [serial online] 2015 2015. Available from: URL: https://www.scopus.com/inward/record.uri?ei*

d=2-s2.0-84925337186&doi=10.1155%2F2015%2F874849&partnerID=40&md5=423db6bd95b29bfff701713658cf0aba

8. *Cheignon C, Tomas M, Bonnefont-Rousselot D, Faller P, Hureau C, and Collin F. Oxidative stress and the amyloid beta peptide in Alzheimer's disease. Redox Biol (2018) 14: 450–464.*
9. *Tang Y, Cui Y, Luo F, Liu X, Wang X, Wu A, et al. Cell viability and dopamine secretion of 6-hydroxydopamine-treated PC12 cells co-cultured with bone marrow-derived mesenchymal stem cells. Neural Regen Res [serial online] 2012 May [cited 2024 Jul 13], 7: 1101. Available from: URL: /pmc/articles/PMC4340024/*
10. *Daubner SC, Le T, and Wang S. Tyrosine Hydroxylase and Regulation of Dopamine Synthesis.*
11. *Teresa Bueno-Carrasco M, Cuéllar J, Flydal MI, Santiago C, Kråkenes T-A, Kleppe R, et al. Structural mechanism for tyrosine hydroxylase inhibition by dopamine and reactivation by Ser40 phosphorylation. [cited 2025 Aug 22]. Available from: URL: https://doi.org/10.1038/s41467-021-27657-y*
12. *Fonseca-Santos B, Gremião MPD, and Chorilli M. Nanotechnology-based drug delivery systems for the treatment of Alzheimer's disease. Int J Nanomedicine (2015) 10: 4981–5003.*
13. *Mani R, Ezhumalai D, Muthusamy G, and Namasivayam E. Neuroprotective effect of biogenically synthesized ZnO nanoparticles against oxidative stress and β-amyloid toxicity in transgenic Caenorhabditis elegans. Biotechnol Appl Biochem [serial online] 2024 February [cited 2025 Aug 22], 71: 132–146. Available from: URL: /doi/pdf/10.1002/bab.2527*
14. *Guo Z, Zhang P, Luo Y, Xie HQ, Chakraborty S, Monikh FA, et al. Intranasal exposure to ZnO nanoparticles induces alterations in cholinergic neurotransmission in rat brain. Nano Today (2020) 35.*
15. *Lv C, Yuan X, Zeng H-W, Liu R-H, and Zhang W-D. Protective effect of cinnamaldehyde against glutamate-induced oxidative stress and apoptosis in PC12 cells. Eur J Pharmacol (2017) 815: 487–494.*
16. *Kim H and Xue X. Detection of Total Reactive Oxygen Species in Adherent Cells by 2',7'-Dichlorodihydrofluorescein Diacetate Staining. J Vis Exp [serial online] 2020 June [cited 2024 Jul 13], 2020: 1–5. Available from: URL: /pmc/articles/PMC7712457/*
17. *Yadav S, Mehrotra GK, and Dutta PK. Chitosan based ZnO nanoparticles loaded gallic-acid films for active food packaging. Food Chem (2021) 334: 127605.*
18. *Azizi-Lalabadi M, Rafiei L, Divband B, and Ehsani A. Active packaging for Salmon stored at refrigerator with Polypropylene nanocomposites containing 4A zeolite, ZnO nanoparticles, and green tea extract. Food Sci Nutr [serial online] 2020 December [cited 2021 Jan 17], 8: 6445–6456. Available from: URL: https://onlinelibrary.wiley.com/doi/10.1002/fsn3.1934*
19. *Alshameri AW and Owais M. Antibacterial and cytotoxic potency of the plant-mediated synthesis of metallic nanoparticles Ag NPs and ZnO NPs: A review. Vol. 8, OpenNano. Elsevier Inc. (2022).*
20. *Park SJ. Protein–Nanoparticle Interaction: Corona Formation and Conformational Changes in Proteins on Nanoparticles. Int J Nanomedicine [serial online] 2020 [cited 2023 Dec 29], 15: 5783. Available from: URL: /pmc/articles/PMC7418457/*